INVESTIGATION OF DIKE-RELATED TOPOGRAPHY AT CRATERS OF THE MOON NATIONAL MONUMENT AND PRESERVE, IDAHO, USING UNPILOTED AERIAL VEHICLES. Melanie B. Callihan[1*], Christian Klimczak[1], Cash A. Owens[1], Roger C. Lowe III[2], Paul K. Byrne[3], [1]Structural Geology and Geomechanics Group, Department of Geology, University of Georgia, 210 Field Street, Athens, GA 30604, *melanie.callihan@uga.edu. [2] Warnell School of Forestry and Natural Sciences, University of Georgia,180 E Green Street, Athens, Ga 30602, [3] Planetary Research Group, Marine, Earth, and Atmospheric Sciences Department, North Carolina State University, 2800 Faucette Drive, Raleigh, North Carolina 27695

Introduction: Field investigations at planetary analogue sites on Earth are key for understanding geologic processes on extraterrestrial worlds. King's Bowl (KB) in Craters of the Moon National Monument and Preserve, Idaho (Fig.1), is an ideal location to test how fractures, pits, and faults are related to intrusion of a shallow or surface-breaching dike. As part of the eastern Snake River plain in southern Idaho, the area has been subjected to rifting and numerous dike-fed volcanic eruptions. Eruptions there in the Holocene have left behind a complex topography characterized by fissures, fractures, pits, and lava flows, making it an excellent analogue for understanding dike-related graben formation on other planets, such as the Moon or Mars, where this process has previously been detected with laser altimeter topographic data [1,2].

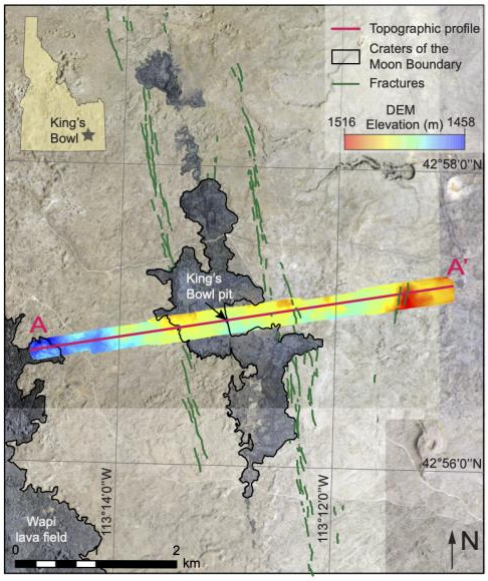

Figure 1. KB rift segment with mapped fractures. The DEM, which covers ~1,680 km^2, reveals a gentle topographic gradient to the east. Topographic profile A–A' strikes through the KB pit.

KB (Fig.1) is located at the southeastern extent of the National Monument and is one of the smallest basaltic fields of the region, with an approximate age of 2220 ± 100 years [3]. The KB rift segment is 12 km long, trending NNW, with a central fissure as indicated by a pit chain, bounded by opening-mode fractures to the east and west. The width of the system is ~1.5 km between the fracture sets.

The fracture formation and eruption has previously been attributed to the intrusion of a shallow subsurface dike [4–6]. The emplacement of shallow dikes is known to cause characteristic ground displacements [7,8], which may be accompanied by contemporaneous or subsequent fracture or fault development [9,10]. On the Moon, graben formation has also been linked to dike intrusion with similar topographic characteristics [1,11]. Rift zones and graben with underlying shallow dikes often present a concave-down topographic profile with pronounced topographic highs at the rims of the rift. This topographic expression can be used to place constraints on the dimensions of subsurface dikes present. Topographic transects between the facture sets at KB rift have been used to quantify local topographic variations that helped constrain dike dimensions [5]. However, this methodology has not yet been applied to the interpretation of the long-wavelength topographic signature of a dike, which reflects large-scale topographic changes beyond the rift zone.

Recent advances in the use of unpiloted aerial vehicles (UAVs) now allow us to collect detailed orthographic imagery, from which we can produce higher-resolution orthomosaics and digital elevation models (DEMs). Using this technology, we show that these high-resolution data products can be used to place constraints on dike dimensions, give insights into fracture formation and preexisting topography, and further enhance our understanding of landform evolution related to dike intrusion with applications to graben on other rocky planets.

Field Methods: To gain a better understanding of long-wavelength topographic ranges along the length of the KB rift we flew multiple ~5 km-long swaths perpendicular to the fissure and fracture zone. These swaths were selected to capture topography beyond the fissure, rift zone, and eruption site, and to encompass areas where lava flows and fracture interaction exist. Orthoimagery was collected using DJI Mavic 2 Pro and DJI Phantom 3 Professional UAVs, flown at varying heights to obtain similar resolutions for the two different cameras. Fig. 1 shows one processed swath, centered on the KB pit. Following Federal Aviation Administration UAV regulations, we used a visual observer to maintain

constant visual contact with the aircraft and split each swath into six individual flights ranging from 0.7 to 1.0 km in length. The swath widths ranged from 240 m to 340 m. Multiple ground control points (GCPs) were placed in the area to aid in the production of high-fidelity georeferenced image products.

Data Processing: The orthographic images collected by the UAVs were processed with Agisoft's Metashape software, merged together to create a large composite orthomosaic and DEM of the area. For the KB swath (Fig.1), we aligned and merged ~3600 images to produce a dense point cloud, from which we then generated the DEM and orthomosaic. 28 GCPs were used across the KB swath resulting in a final resolution of 2.8 cm/px for the orthomosaic and DEM (Fig. 2).

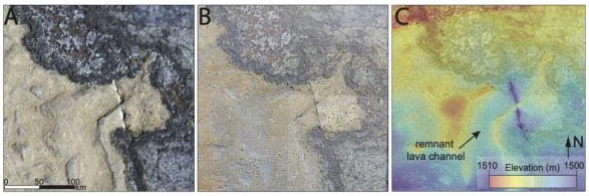

Figure 2. Comparison of existing and new data products. Existing National Agricultural Image Program orthoimagery at 1-meter resolution (A). B and C show data collected by this study at 2.8 cm/px resolution, revealing unprecedented detail in the orthomosaic and topographic variations in the DEM.

Results: The orthomosaics produced in this study so far, together with our field observations, revealed three fractures within the lava flow near KB pit that have previously been undetected in existing orthoimagery. Additionally, the newly generated DEMs show very detailed variations in topography and capture older lava flow morphologies, such as a remnant lava channel (Fig. 2C), which may have influenced recent fracture formation and lava flows.

We extracted topographic profile A–A' across the area, centered on the KB pit (Fig. 3). The observed topographic profile shows an overall change in elevation of 25 m, reflecting an increase towards the east, and lower topography towards the west, near the Wapi lava field. We observe a topographic rise near the central fissure of ~6 m above the surrounding terrain with a width of 1.9 km. We compared these regions to the extent of the existing lava flow and determined that the rise was not caused by inflated lava flows. The topography of the rift also appears symmetrical about the rift center and displays a depression near the KB pit. In detrending the profile, it also becomes apparent that fractures are located at the highest points along the subtle rises that parallel the rift itself and the flank profiles to the east and west appear concave down. We interpret that this topographic rise and surrounding features are caused by a shallow or surface-breaking dike.

Outlook: We additionally collected two similar swaths across the north and south KB rift zone. Further analysis will allow us to constrain if and how dike dimensions vary across the rift, and if preexisting topography influenced fracture and rift formation.

We plan on modeling dike-related topography to infer dike geometries, including dike aperture, length, and height, along all our swaths and comparing the results to previous findings of shallow dike intrusions, which used a combination of buoyancy equilibrium and boundary element models [5.] Furthermore, our observations will help constrain timing relationships between fracturing, eruption, and pit formation. A better understanding of geometric properties and dimensions of the dike intrusion resulting from this study can also be applied to lunar graben, especially to those that share morphological characteristics of the KB rift zone and pit crater chains.

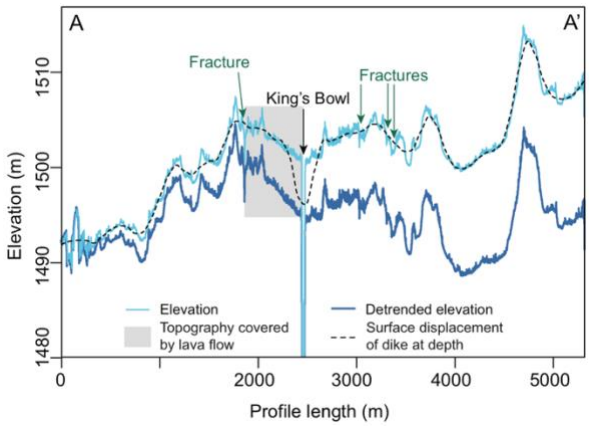

Figure 3. Observed and detrended topographic profiles across KB shown in light and dark blue, respectively. The average surface displacement (black dashed line) highlights typically observed topographic profile for shallow dike intrusion.

References: [1] Klimczak, C. (2014) *Geology* 42, 963–966. [2] Schultz, R. A. et al. (2004), *Geology* 32, 889–892 [3] Kuntz, M. A (1992). *Reg. Geol. East. Idaho & West. Wyoming* 179, 289–304 (1992). [4] Kuntz, M. A. et al. (2002) *Spec. Pap. 353*, 111–133. [5] Holmes, A. A., et al. (2008) *JGR* 113, 15379–15 (2008). [6] Hughes, S. S. *et al.* (2018) *J. Volcanol. Geoth. Res.* 351, 89–104. [7] Pollard, D. D., et al (1983) *Tectonophysics* 94, 541–584. [8] Mastin, L. G. & Pollard, D. D. (1988) *JGR* 93, 13221–13235. [9] Rubin, A. M. & Pollard, D. D. (1988) *Geology* 16, 413-417. [10] Rubin, A. M. (1992) *JGR* 97, 1839–1858. [11] Head, J. W. and Wilson, L. (1992) *Geochim. Cosmochim. Ac.* 56, 2155–2175.